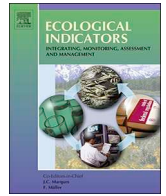




ELSEVIER

Contents lists available at ScienceDirect

Ecological Indicators

journal homepage: www.elsevier.com/locate/ecolind

Land use/cover predictions incorporating ecological security for the Yangtze River Delta region, China

Dou Zhang^a, Xiangrong Wang^{a,*}, Liping Qu^b, Shicheng Li^{b,c}, Yuanping Lin^b, Rui Yao^d, Xiao Zhou^b, Jingye Li^b

^a Department of Environmental Science and Engineering, Fudan University, Shanghai 200438, China

^b School of Public Administration, China University of Geosciences, Wuhan 430074, China

^c Key Laboratory of Meteorological Disaster of Ministry of Education, Nanjing University of Information Science and Technology, Nanjing 210044, China

^d Hubei Key Laboratory of Critical Zone Evolution, School of Geography and Information Engineering, China University of Geosciences, Wuhan 430074, China

ARTICLE INFO

Keywords:

Ecological security source areas (ESSA)
Scenarios simulation
Land use prediction
FLUS model
The Yangtze River Delta

ABSTRACT

Rapid changes in anthropogenic land use threaten ecological security; thus, it is vital to determine future land use structures and spatial layouts for ecological security and sustainable development. Studies on scenario-based land use simulations have taken insufficient account of land use in terms of ecological security and this prevented the realization of ecological civilization. Therefore, in this study, we developed a land use/cover prediction framework that incorporates ecological security. Focusing on ecological security objectives, we integrated habitat quality, the importance of ecosystem services and landscape connectivity to identify the ecological security source areas (ESSA) as a minimum protection area in the Yangtze River Delta (YRD) region. We then set up ESSA-based ecological protection (EP) and natural growth (NG) scenarios to predict land use/cover in the YRD region for 2030 using the future land use simulation (FLUS) model. The results show that the total area of the ESSA is 64,911 km², accounting for 32.51% of the YRD, mainly in southern Anhui and western Zhejiang provinces. Under the NG scenario, construction land shows the highest growth proportion by 2.10% of the total area of YRD, while the farmland area decreases by 1.73%, followed by woodland (0.27%). Under ESSA-based EP, the areas of woodland and construction land increase by 1.11% and 0.7%, respectively. Through the delineation of ESSA, 159 km² of woodland, 150 km² of orchard, 523 km² of water area and 98 km² of wetland are protected; in addition, the growth of the construction land slows down and all new construction land is located outside the ESSA under ESSA-based EP. The findings of this study can provide fundamental scientific guidance for land spatial planning given an ecological security premise.

1. Introduction

Human activities continuously change the land use/cover in the world leading to decreased stability of ecosystems and threatening ecological security (Wood et al., 2018). Over the past half-century, with dramatically increasing global population and rapid urbanization, the structure and function of ecosystems have been greatly disturbed by human land use activities and therefore experienced unprecedented changes (Costanza et al., 2014; Geijzendorffer et al., 2017). These land use activities resulted in various environmental problems including soil erosion, biodiversity loss and water pollution, threatening global ecological security and sustainable development (Li et al., 2019; Yao et al., 2019). The optimization of land use patterns to reduce the impact of land use changes on ecosystems and ensure regional ecological security

has thus become a research hotspot (Jin et al., 2019, 2018; Ma et al., 2019).

In recent years, China has showed great progress in economic development, but the conflict between anthropogenic land use and ecological protection has also increased significantly (Li et al., 2018; Qiu et al., 2019). To overcome the eco-environmental problems caused by human activities, China has raised the implementation of ecological-security-related policies to the national strategy level (Jiang et al., 2019; Wang et al., 2019). With rapid economic development and urbanization, the Yangtze River Delta (YRD) region has experienced severe eco-environmental degradation while realizing rapid economic growth. Therefore, exploring the spatial planning of land under the constraint of ecological security in the YRD is of great significance in terms of providing guidance for other regions in China.

* Corresponding author.

E-mail address: rxrwang@fudan.edu.cn (X. Wang).

<https://doi.org/10.1016/j.ecolind.2020.106841>

Received 28 October 2019; Received in revised form 9 June 2020; Accepted 10 August 2020

1470-160X/© 2020 Elsevier Ltd. All rights reserved.

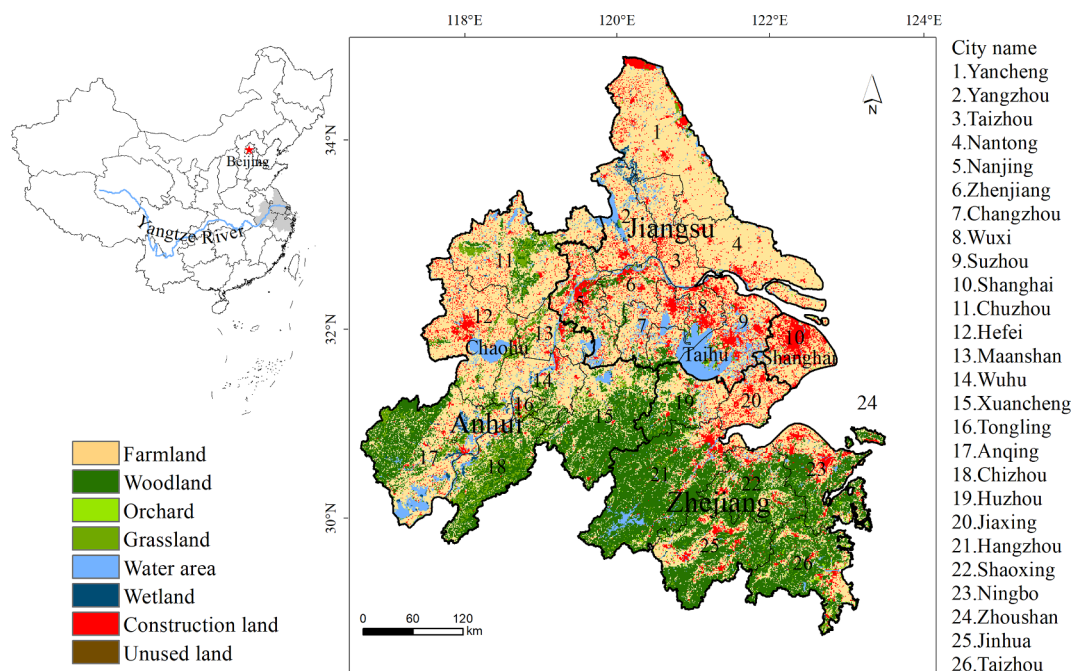


Fig. 1. Location and land use pattern of the Yangtze River Delta region in 2015.

Land use/cover change is a result of multiple interacting processes driven by socioeconomic and biophysical factors and has significant impacts on the ecological environment (Lin et al., 2014; Verburg et al., 2002). Exploring the competition and evolution among land use types and predicting future land use changes can help optimize land use patterns and improve the ecological environmental quality (Liu et al., 2011; Luo et al., 2014). Various models have been developed and applied to predict future land use patterns, such as cellular automata (Kang et al., 2019), conversion of land use and its effects (CLUE) model (Zhou et al., 2016) and agent-based models (Teng et al., 2011). Recently, a new model, the future land use simulation (FLUS) model, has been proposed to simulate the long-term changes in multiple land use types simultaneously by coupling human and natural systems (Liu et al., 2017). Compared with the previous models, the FLUS model not only improves the calculation process of the probability of occurrence by using artificial neural networks (ANNs), but also elaborate conversion among different land use types with a self-adaptive inertia and competition mechanism (Liang et al., 2018). ANNs have been proved to be a more effective tool than logistic regression, which is the core of the CLUE model to manage complex nonlinear relationships between different land use types and their driving factors (Islam et al., 2018; Kadavi and Lee, 2018). The FLUS model makes it more convenient to simulate land use by utilizing complex geographic, socio-economic and climatic conditions.

Existing models do not adequately consider ecological security when simulating future land use patterns. Most previous studies directly selected nature reserves and rivers as spatial restricted areas for ecological protection, ignoring the role of ecosystem services and landscape integrity in safeguarding ecological security. For example, Teng et al. (Teng et al., 2011) simply designated nature reserves, rivers and reservoirs as constrained areas to simulate urban expansion. Wang et al. (Wang et al., 2018) selected nature reserves and the Yangtze River Delta as restricted areas to project land use changes for ecological protection. Ecological security can be defined as the state of the ecological environment where the safety of human life and production, as well as the ability to adapt to environmental changes, is guaranteed (Huang et al., 2007; Liu and Chang, 2015). The goals of ecological security include preventing ecological degradation, maintaining the sustainability of ecosystem services and maintaining landscape

integrity (Wu et al., 2013). Compared with the existing protected areas, ecological security source areas (ESSA) are considered effective pathways to guarantee ecological security (Peng et al., 2018; Zhang et al., 2016). ESSA refer to the sources of biological movements and ecosystem service flows and transmissions, which play a key role in overall ecosystem health and are essential to achieve regional ecological security (Yu et al., 2009). In recent years, the identification of ESSA has experienced rapid development and is achieved using three main methods: (1) direct selection of forest land or nature reserves (Teng et al., 2011; Yao and Xie, 2016); (2) selection of ecological patches with a large supply of ecosystem services (Shi and Yu, 2014); and (3) building a comprehensive index system to evaluate the importance of ecological patches (Kong et al., 2010). Nevertheless, only a few studies have identified ESSA based on habitat quality, ecosystem services and landscape connectivity simultaneously, which correspond to three goals of ecological security.

In this study, we propose a land use/cover prediction framework that incorporates ecological security by coupling the comprehensive evaluation of ESSA and using the FLUS model. The ESSA evaluation can help us find where ESSA should be strictly protected. The land use/cover prediction under the constraints of ESSA can guide regional spatial planning by balancing ecological protection and anthropogenic land use. The main objectives of this study are to (1) address ecological security and identify ESSA by performing an assessment of habitat quality, ecosystem services and landscape connectivity; (2) simulate and predict future land use patterns constrained by ESSA using the FLUS model; (3) compare and analyze the land use changes under ESSA-based EP with NG scenarios.

2. Study area and data sources

2.1. Study area

The YRD region encompasses 26 cities in China (Shanghai, nine cities in Jiangsu Province, eight in Zhejiang Province and eight in Anhui Province) (Fig. 1). It is located in a subtropical monsoon climate zone downstream of the Yangtze River (115°46' E–123°25' E, 29°20'–32°34' N). Total annual precipitation ranges between 800 and 1600 mm. The landform of the study area is dominated by the Taihu Plain, with an

Table 1

Data information and sources. DEM = digital elevation model; NDVI = normalized difference vegetation difference; NPP = net primary productivity; GDP = gross domestic product.

| Data Name | Resolution | Time | Data Source |
|--------------------------------------|-------------|-----------|---|
| Vegetation type | 1 km | 1980 | Chinese Academy of Sciences Data Center for Resources and Environmental Sciences (http://www.resdc.cn) |
| Soil type | 1 km | 1995 | |
| DEM | 90 m | 2003 | |
| Nighttime light image | 1 km | 2013 | |
| Land use/cover | 1 km | 2010/2015 | |
| Precipitation | 1 km | 2015 | |
| Temperature | 1 km | 2015 | |
| NDVI | 1 km | 2015 | |
| NPP | 1 km | 2015 | |
| Administrative boundary | City/county | 2015 | |
| GDP | 1 km | 2015 | |
| Population | 1 km | 2015 | Specimen Resource Sharing Platform of China Nature Reserve (http://www.papc.cn/) Science and Technology Resource Service System of National Ecosystem Observation and Research Network (http://www.cnerm.org.cn/) |
| Nature reserves | - | 2015 | |
| Perennial average evapotranspiration | 1 km | 1961–2000 | |

elevation of less than 10 m, and low hills in the southwest and south. The total area of the region is 211,700 km², accounting for 2.21% of China. As one of the most dynamic regions of rapid economic development in China, the YRD region faces severe environmental degradation and deterioration of ecosystem functions.

2.2. Data sources

The basic data used in this study and the data sources are listed in Table 1. The land use data were generated via the interpretation of remote sensing data and visual interpretation of Landsat 8 remote sensing images. The annual average temperature and precipitation data were generated based on the collation, calculation and spatial interpolation of daily observations from over 2400 meteorological stations in China, in units of 0.1 °C and 0.1 mm, respectively.

3. Methods

The general structure of the proposed framework is illustrated in Fig. 2 and involves three main technical steps. First, ESSA were identified through a comprehensive evaluation system consisting of habitat quality, the importance of ecosystem services, and landscape

connectivity. Second, the Markov model was used to project the demand area of each land use type in 2030. Third, the FLUS model was used to predict the land use patterns in 2030 for ESSA-based EP and NG scenarios. The land use pattern in the EP scenario is constrained by ESSA through complex processes of competition and interactions among different land use types. The simulation under NG was conducted to perform a comparative analysis with ESSA-based EP and to illustrate the importance and necessity of land use predictions that incorporate ecological security.

3.1. Identification of ecological security source areas

ESSA are the main areas where regional ecological security is maintained for the overall stability and continuity of regional ecosystems. ESSA should not only have important ecosystem services, but also have high habitat quality to prevent ecological degradation and the ability to maintain landscape connectivity (Peng et al., 2018). Therefore, we constructed a comprehensive evaluation method to identify ESSA based on the habitat quality, ecosystem services and landscape connectivity. The weights of these three indicators obtained using the Delphi method are 0.25, 0.50 and 0.25, respectively. The results were standardized to five classes using the Jenks natural breaks classification

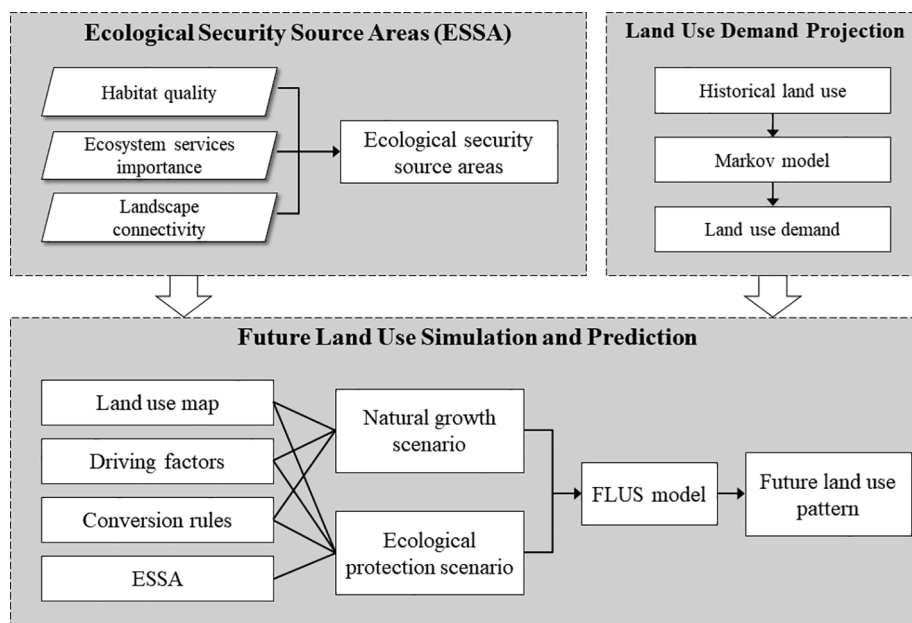


Fig. 2. The framework of land use prediction incorporating ecological security.

Table 2
Habitat quality assessment parameters in YRD region.

| Threat source | Weight | Sensitivity Farmland | Woodland | Grassland | Water area | Wetland | Maximum influence distance (km) |
|--------------------------|--------|-------------------------|----------|-----------|------------|---------|---------------------------------|
| Human activity intensity | 1 | 0.75 | 0.75 | 0.5 | 0.8 | 0.8 | 10 |
| Highway | 0.8 | 0.8 | 0.65 | 0.3 | 0.65 | 0.7 | 3 |
| Railway | 1 | 0.5 | 0.55 | 0.2 | 0.55 | 0.6 | 5 |
| Port | 1 | 0.5 | 0.8 | 0.8 | 0.8 | 0.8 | 10 |
| Channel | 0.8 | 0.5 | 0.7 | 0.7 | 0.7 | 0.75 | 3 |

method in ArcGIS 10.2, which can maximize the differences between the classes. Two classes with the highest scores were selected as ESSA (Guo et al., 2019).

3.1.1. Habitat quality

Habitat quality refers to the ability of an ecosystem to provide sustainable living conditions for individuals and a community based on the availability of resources (Hall et al., 1997). Habitat quality generally decreases with as nearby land use intensity increases (Petrosillo et al., 2009). The Integrated Valuation of Ecosystem Services and Tradeoffs (InVEST) tool has been widely employed to estimate the habitat quality (Posner et al., 2016). Habitat quality is calculated as follows:

$$Q_{xj} = H_j \left[1 - \left(\frac{D_{xj}^z}{D_{xj}^z + k^z} \right) \right] \quad (1)$$

where Q_{xj} is the habitat suitability; k is the subsaturation constant, generally a half of the maximum value of D_{xj} ; and z is a constant. The parameter settings in the model are presented in Table 2. The intensity of human activity is expressed using the nighttime light index.

3.1.2. Importance of ecosystem services

The importance of ecosystem services is evaluated to determine the critical positions, which are extremely important to regional ecosystems based on the analysis of the main ecosystem services and ecological processes (Li et al., 2013). Based on the major ecological problems in the YRD region, the importance of ecosystem services was evaluated by spatially integrating the water yield, soil conservation and biodiversity conservation with the weights of 0.3, 0.3 and 0.4 respectively (Li et al., 2020; Peng et al., 2018).

The water yield service was calculated using the water balance equation, and the surface runoff coefficient was taken from a previous study (Gong et al., 2017).

$$TQ = \sum_{i=1}^j (P_i - R_i - ET_i) \times A_i \quad (2)$$

where TQ is the annual water yield, m^3 ; P_i is the annual precipitation, mm ; R_i is the surface runoff, mm ; ET_i is the evapotranspiration, mm ; A_i is the area of i ecosystem, m^2 ; i is the type of ecosystem; and j is the number of ecosystem types.

Soil conservation service was estimated using the revised general soil erosion equation (RUSLE) (Xiao et al., 2015).

$$A_c = R \times K \times LS \times (1 - C \times P) \quad (3)$$

where A_c is the annual amount of soil conservation, $t/hm^2 a$; R is the rainfall erosivity factor, $MJ mm/hm^2 h a$; K is the soil erodibility factor, $t hm^2 h/MJ hm^2 mm$; LS is the slope length and steepness factor; C is the vegetation coverage factor; P is the factor of engineering conservation measures.

Biodiversity conservation service was evaluated using the method of landscape security pattern (Hu et al., 2010). First, we selected 30 national and provincial nature reserves in the YRD region as sources of biodiversity conservation. Then, the integrated resistance surface was constructed by normalizing the resistance factors such as slope, net primary productivity (NPP) and nighttime light index. Finally, we

obtained the spatial cost distance of the biological movements using the minimum cumulative resistance model, which reflects the importance of biodiversity conservation. Boundaries of different importance levels were identified based on the relationship between the distance from the sources and the accumulated resistance value.

3.1.3. Landscape connectivity

The level of landscape connectivity within the region can quantitatively characterize whether a certain landscape type is suitable for species exchange and migration and this is important for the biodiversity conservation and ecosystem balance (Saura and Pascual-Hortal, 2007). Morphological spatial pattern analysis (MSPA) is a method that uses mathematical morphological operations to identify areas important for landscape connectivity at the pixel level (Soille and Vogt, 2009; Velázquez et al., 2017). We identified and extracted the core area from the entire landscape using the MSPA in the Guidos Toolbox. Then, we used the probability of connectivity (PC) index to evaluate the landscape connectivity of the core area using the software Conefor 2.6 (Saura and Pascual-Hortal, 2007). The higher the value of PC, the better the landscape connectivity.

$$PC = \frac{\sum_{i=1}^n \sum_{j=1}^n a_i \times a_j \times p_{ij}^*}{A_L^2} \quad (4)$$

where A_L is the total area of the landscape; a_i and a_j are the areas of ecological patches i and j , respectively; p_{ij} is the maximum connectivity value of all paths between patches i and j ; and n is the number of patches.

3.2. Land use demand area projection

To better understand the impact of ecological protection on future land use, the NG and ESSA-based EP scenarios were designed in this study. The NG scenario follows the historical trend of land use change and does not apply any policy to alter original land use changes. Considering the time series as a random process, the Markov model determines the trends to make predictions by studying the initial probability of different states of land use and the probability of conversion between the states (Aburas et al., 2017; Lu et al., 2018). Therefore, a Markov model was used here to predict the demand area for each land use type in 2030 based on the historical land use data in 2010 and 2015 for the NG scenario.

The ESSA-based EP scenario aims to protect important ecological areas with specific location and ecosystem functions to maintain regional ecological security. According to the "Development Plan of Yangtze River Delta Urban Agglomerations from 2010 to 2030" (DP-YRD) (Commission, 2016), the local government is planning to implement stricter ecological protection policies. Hence, in the ESSA-based EP scenario, we set the area of the status quo ($55,070 km^2$) as the lower-bound value of the woodland area required to protect the forest ecosystem. The water and wetland area should be equal to the corresponding area in the status quo, $13,912 km^2$ and $1563 km^2$, respectively, to ensure water security. As the development intensity of the land in the YRD region reached 17.1% in 2013, higher than the level of 15% of the Pacific coastal agglomeration in Japan, the space potential

for follow-up construction is insufficient. To control the intensity of the development of construction land and improve the efficiency with which territorial space is utilized, construction land in 2030 should be less than the area predicted in 2020 based on the Markov model (25,486 km²) and greater than the status quo (23,655 km²).

3.3. Land use allocation based on the FLUS model

The FLUS model consists of two modules: (1) an ANN used to train and calculate the probability of occurrence of each land use type on a specific grid, and (2) an elaborated self-adaptive inertia and competition mechanism for analyzing the competition and interactions among multiple land use types. The optimal land use type is allocated to each grid until the quantity of each land use type reaches the predicted demand.

3.3.1. Driving factors of land use changes

In the first module, 12 spatial variables were selected to calculate the probability of occurrence. The natural environment factors include elevation, topographical relief and normalized difference vegetation difference (NDVI). The climate factors include precipitation and temperature. The socio-economic factors include nighttime light index, GDP and population per grid. The distance factors include the distance to urban centers, county centers, railways and rivers, which are generated using the Euclidean distance tool in ArcGIS. Based on the land use data in 2015 and multiple input variables, the ANN approach was applied by random sampling training and with 10% sample proportion.

3.3.2. Spatial constraints and conversion settings

In the second module, different from the traditional method of directly designating nature reserves and scenic spots as spatial constraints, this study designates ESSA as spatial constraints in the ESSA-based EP. For the NG scenario, there are no spatial constraints. In addition, two parameters need to be provided for a self-adaptive inertia and competition process. The neighborhood effect refers to the difficulty degree of the conversion from one land use type to another. The closer the neighborhood effect is to 1, the stronger the expansion capacity of the land use type is. The neighborhood effect for each land use type is determined based on the expert knowledge and the related literature (Liang et al., 2018; Liu et al., 2017) (Table 3). The conversion constraint matrix describes the permission of the conversion from one land use type to another. In the matrix, “1” denotes possible conversion and “0” denotes the opposite. The conversion constraint matrices are illustrated in Fig. 3.

3.3.3. Model validation

We used the kappa coefficient to evaluate the performance of the FLUS model. Generally, the kappa coefficient ranging between 0.6 and 0.8 represents high simulation consistency, while 0.8–1.0 represents nearly complete consistency. Land use data in 2010 were regarded as the initial state to obtain the predicted land use in 2015 using the FLUS model. By comparing the real land use image in 2015 with the predicted land use map in 2015, we show that overall accuracy of the simulation is 87.83% and the individual accuracy levels for farmland, woodland, grassland and wetland are higher than 89% (Table 4). The kappa coefficient of eight land use types is 0.82. The validation results

Table 3
The neighborhood effect of each land use type under NG and ESSA-based EP.

| Scenario | Farmland | Woodland | Orchard | Grassland | Water area | Wetland | Construction land | Unused land |
|-----------------------|----------|----------|---------|-----------|------------|---------|-------------------|-------------|
| Natural growth | 0.5 | 0.8 | 0.4 | 0.3 | 0.5 | 0.4 | 1 | 0.3 |
| Ecological protection | 0.6 | 0.9 | 0.5 | 0.4 | 0.7 | 0.5 | 0.8 | 0.3 |

show that the FLUS model have high simulation accuracy when applied to the YRD region. Therefore, its reliability in predicting future land use change with validated parameters is also high.

4. Results

4.1. Ecological security source areas

High-quality habitats are mainly located to the south of the YRD, in mountainous and hilly areas in the west, and around Taihu and Chaohu lakes (Fig. 4a). Areas with a high ecosystem service value are mainly located in western Zhejiang and southern Anhui (Fig. 4b). Areas with high landscape connectivity are mainly located in the southern and central YRD, accounting for 38.36% of the total area, which indicates that overall regional landscape connectivity is high (Fig. 4c).

The total area of ESSA in the YRD region is 64,911 km², accounting for 32.51% of the entire area (Fig. 4d). ESSA are distributed in southern and western Anhui, in the mountainous and hilly areas, central and western Zhejiang, as well as Taihu and Chaohu lakes, which are located in the cities of Anqing, Chizhou, Xuancheng, Huzhou, Hangzhou, Jinhua, Shaoxing and Taizhou. In terms of land use types, ESSA are mainly composed of woodland, water area and wetland, followed by farmland and grassland. These areas not only have high forest coverage and high ecological services provision, such as water yield, soil retention and biodiversity conservation, but also are located in high altitudes.

To verify the identification result of ESSA, we compared ESSA with the existing national and provincial natural reserves in the YRD region. Based on this data, the distribution of all national and provincial nature reserves nearly overlaps the distribution of ESSA. Fig. 5 shows that most of the thirty national and provincial nature reserves are located within the ESSA, indicating the viability of the ESSA identification method.

4.2. Temporal land use change for 2015–2030

In 2015 data, the farmland accounts for 49.98% of the total land area in the YRD, followed by woodland (26.82%) and construction land (11.52%). The total area of farmland, woodland, orchard and grassland accounts for nearly 81%, while the area of water and wetlands only account for 7.46% in the YRD. Table 5 lists land use change under the two scenarios from 2015 to 2030. Under NG, the area of the construction land increased by 4314 km². The area of the farmland decreased by 3553 km², followed by woodlands and wetlands with the decrease of 547 km² and 122 km², respectively.

However, under the ESSA-based EP scenario, ESSA cannot be occupied and woodland conversion is more stringent, as shown previously in Fig. 3. Therefore, Woodlands showed the opposite trend compared to that in the NG scenario; the area of woodlands increased by 2278 km². The area of the farmland decreased by 931 km², which is also in line with China's farmland protection policy. The largest drop occurred in the area of grasslands (2105 km²). Besides, water and wetland areas remained stable under the ESSA-based EP. In general, under the ESSA-based EP, the growth of the construction land slows down while woodland, wetland and water areas are effectively protected.

The land use conversion matrix obtained with the Markov model was used to explore the land conversion process under two scenarios

| | | | | | | | | |
|----------|--------------------------------|----------|----------|----------|----------|----------|----------|----------|
| | 1 | 2 | 3 | 4 | 5 | 6 | 7 | 8 |
| 1 | 1 | 1 | 1 | 1 | 1 | 1 | 1 | 1 |
| 2 | 1 | 1 | 1 | 1 | 0 | 0 | 1 | 1 |
| 3 | 1 | 1 | 1 | 1 | 0 | 0 | 1 | 1 |
| 4 | 1 | 1 | 1 | 1 | 1 | 1 | 1 | 1 |
| 5 | 1 | 1 | 1 | 1 | 1 | 1 | 1 | 1 |
| 6 | 1 | 1 | 1 | 1 | 1 | 1 | 1 | 1 |
| 7 | 0 | 0 | 0 | 0 | 0 | 0 | 1 | 0 |
| 8 | 1 | 1 | 1 | 1 | 1 | 1 | 1 | 1 |
| | Natural growth scenario | | | | | | | |
| | 1 | 2 | 3 | 4 | 5 | 6 | 7 | 8 |
| 1 | 1 | 1 | 1 | 1 | 1 | 1 | 1 | 0 |
| 2 | 0 | 1 | 1 | 1 | 0 | 0 | 0 | 0 |
| 3 | 1 | 1 | 1 | 1 | 0 | 0 | 1 | 0 |
| 4 | 1 | 1 | 1 | 1 | 1 | 1 | 1 | 0 |
| 5 | 0 | 1 | 0 | 0 | 1 | 1 | 0 | 0 |
| 6 | 0 | 1 | 0 | 0 | 1 | 1 | 0 | 0 |
| 7 | 0 | 0 | 0 | 0 | 0 | 0 | 1 | 0 |
| 8 | 1 | 1 | 1 | 1 | 1 | 1 | 1 | 1 |
| | Ecological protection scenario | | | | | | | |

Fig. 3. The conversion constraint matrix under natural growth and ecological protection scenarios (codes 1–8 in bold represent farmland, woodland, orchard, grassland, water area, wetland, construction land and unused land respectively).

Table 4
The validation results of the FLUS model in the Yangtze River Delta region.

| Land use type | User's accuracy | Overall accuracy | Kappa coefficient |
|-------------------|-----------------|------------------|-------------------|
| Farmland | 0.904024 | 0.878336 | 0.815876 |
| Woodland | 0.895974 | | |
| Orchard | 0.483221 | | |
| Grassland | 0.897931 | | |
| Water area | 0.868035 | | |
| Wetland | 0.895425 | | |
| Construction land | 0.751993 | | |
| Unused land | 0.500000 | | |

(Table 6). Under the NG scenario, the interchange between various land uses are more obvious and intense. The changed land accounts for 9.86% of the total land area under NG; however, under ESSA-based EP, the ratio is only 3.35%. This indicates a more stable and orderly change in land use.

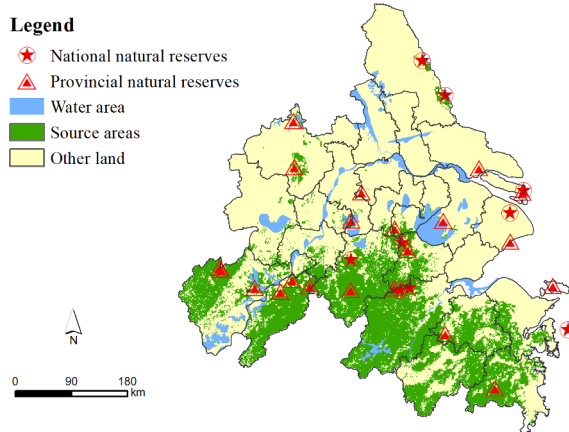


Fig. 5. Spatial overlap between nature reserves and ecological security source areas in the YRD region.

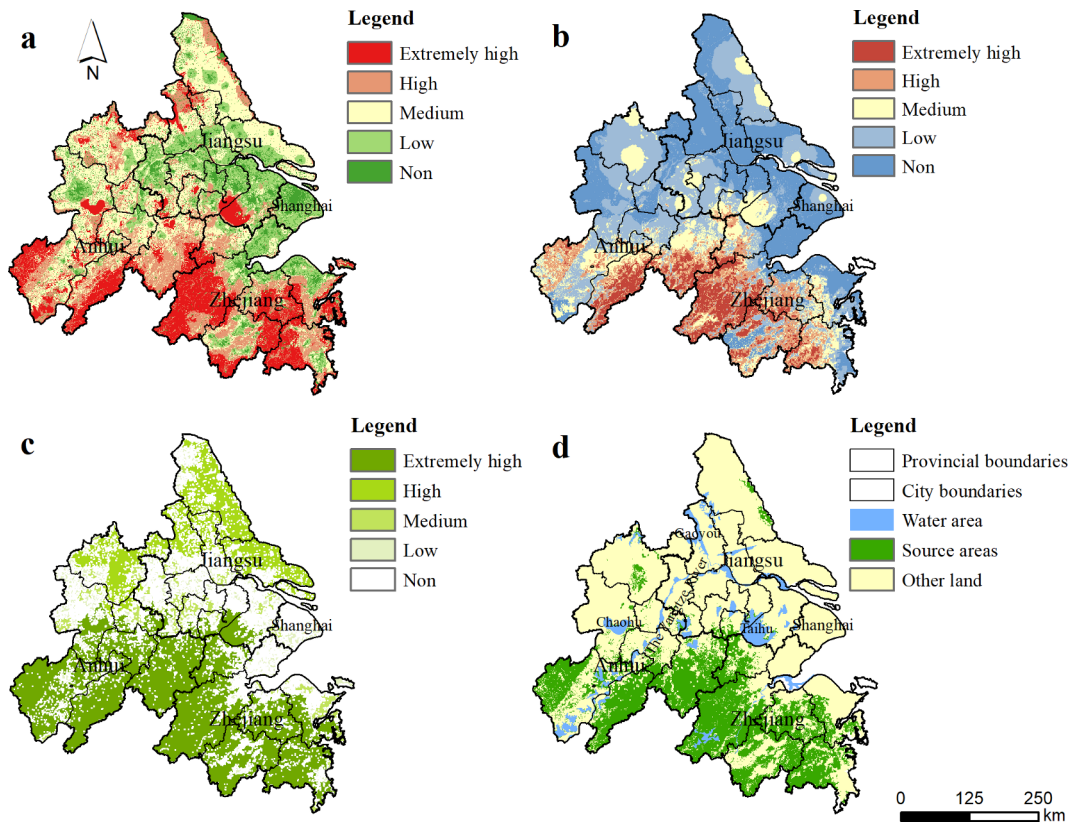


Fig. 4. Ecological security source areas in the YRD region. (a. habitat quality; b. ecosystem services importance; c. landscape connectivity; d. ecological security source areas).

Table 5
Land use change for 2015–2030 under natural growth (NG) and ecological protection (EP) scenarios.

| Land use type | Area (km ²) | | Proportion (%) | | | Change (%) | | |
|-------------------|-------------------------|-----------|----------------|-------|-----------|------------|-------|-------|
| | 2015 | 2030 (NG) | 2030 (EP) | 2015 | 2030 (NG) | 2030 (EP) | NG | EP |
| Farmland | 102,627 | 99,034 | 101,696 | 49.98 | 48.25 | 49.53 | -1.73 | -0.45 |
| Woodland | 55,070 | 54,523 | 57,348 | 26.82 | 26.55 | 27.93 | -0.27 | 1.11 |
| Orchard | 1315 | 1285 | 679 | 0.64 | 0.63 | 0.33 | -0.01 | -0.31 |
| Grassland | 7133 | 7112 | 5028 | 3.47 | 3.46 | 2.45 | -0.01 | -1.03 |
| Water area | 13,912 | 13,879 | 13,912 | 6.78 | 6.76 | 6.78 | -0.02 | 0.00 |
| Wetland | 1563 | 1441 | 1563 | 0.76 | 0.70 | 0.76 | -0.06 | 0.00 |
| Construction land | 23,655 | 27,969 | 25,085 | 11.52 | 13.62 | 12.22 | 2.10 | 0.70 |
| Unused land | 51 | 83 | 15 | 0.02 | 0.02 | 0.01 | 0.00 | -0.02 |

4.3. Spatial changes in land use in 2015–2030

Fig. 6 displays the land use patterns in 2030 for two scenarios. In both scenarios, construction lands in the YRD region are mainly located in Shanghai, western Jiangsu and northern Zhejiang. Woodlands are concentrated in the south of the YRD region, while farmlands are widely distributed in the north and west of the YRD region. To analyze the spatial characteristics of land use changes, changes in four major land use types from 2015 to 2030 under two scenarios were extracted for visualization (Fig. 6).

The decrease in the area of farmlands mainly distributed along the Yangtze River in the NG scenario is more than that in the ESSA-based EP scenario. Woodlands present a completely opposite spatial change trend under NG and ESSA-based EP. The former shows a reduction in the south of the study area, while the latter shows an increase in the west of study area. Similar to farmlands, water areas experience a significant decrease under NG. However, water areas remain unchanged under ESSA-based EP due to the strict constraints on land use. Under NG, construction land shows an expansion at the cost of loss of farmlands, concentrated in the east of the study area. On the contrary, the expansion degree of the construction land is much lower under ESSA-based EP. The Fig. 6 shows that construction land expansion is restrained in rapidly developing areas such as Shanghai and Suzhou under the ESSA-based EP.

4.4. Land use occupying ecological security source areas

Under the NG scenario, the areas of farmland, woodland, orchard, grassland, water bodies and wetland are 8958, 44286, 458, 4780, 5856 and 467 km², respectively, in the area designated as ESSA. Under the ESSA-based EP scenario, the land use type in ESSA remains the same as the land use status in 2015. The areas of farmland, woodland, orchard, grassland, water bodies and wetland are 8097, 44445, 608, 4718, 6379

and 565 km², respectively. Thus, under the ESSA-based EP scenario, 159 km² of woodland, 150 km² of orchard, 523 km² of water area and 98 km² of wetland are protected in ESSA while 861 km² of farmland and 60 km² of grassland are replaced with other types of ecological land.

We further extracted the new construction land data for 2015–2030 under the two scenarios and overlaid them with the distribution map of ESSA (Fig. 7). Under the NG scenario, new construction land is widely distributed around the towns in the center and east of the study area. There is 8 km² of new construction land occupying the ESSA, which is scattered in the southeast of the YRD region. Under ESSA-based EP, new construction land is reduced to 1430 km², all of which is located outside the ESSA and mainly distributed in the northwest of the study area. The results show that ESSA-based EP has a positive impact on ecological environmental protection, and the land use pattern under ESSA-based EP is more conducive to regional ecological security.

5. Discussion

5.1. Limitations

The first limitation of this study is related to the indicators of ecosystem services. Three ecosystem services concerning water, soil and biology were valued and mapped in this study. However, other important services that also likely provide a large value to the society, such as carbon storage, agriculture production and marine ecosystem services were not considered. In summary, the evaluation results in this study do not completely reflect the local ecosystem services capacity and values. There are ubiquitous trade-offs between provisioning services and other types of services found in the Millennium Ecosystem Assessment (2005), which means we should simultaneously consider multiple local services and correctly assess the existence and magnitude of trade-offs. Only this way, decision-makers can formulate rational

Table 6
Land use conversion matrix for 2015–2030 under natural growth (NG) and ecological protection (EP) (area unit: km²).

| Scenarios | 2030 2015 | Farmland | Woodland | Orchard | Grassland | Waterarea | Wetland | Construction land | Unused land |
|-----------|-------------------|----------|----------|---------|-----------|-----------|---------|-------------------|-------------|
| NG | Farmland | — | 1824 | 469 | 143 | 4156 | 398 | 4034 | 3 |
| | Woodland | 1960 | — | 22 | 336 | 54 | 3 | 172 | 0 |
| | Orchard | 554 | 2 | — | 0 | 19 | 0 | 8 | 0 |
| | Grassland | 257 | 165 | 0 | — | 60 | 3 | 24 | 0 |
| | Water area | 4208 | 3 | 59 | 8 | — | 353 | 67 | 0 |
| | Wetland | 492 | 1 | 3 | 1 | 375 | — | 7 | 0 |
| | Construction land | 0 | 0 | 0 | 0 | 0 | 0 | — | 0 |
| EP | Unused land | 3 | 5 | 0 | 0 | 1 | 0 | 2 | — |
| | Farmland | — | 2342 | 3 | 26 | 0 | 0 | 1375 | 0 |
| | Woodland | 310 | — | 2 | 6 | 0 | 0 | 0 | 0 |
| | Orchard | 611 | 12 | — | 0 | 0 | 0 | 18 | 0 |
| | Grassland | 1869 | 232 | 0 | — | 0 | 0 | 36 | 0 |
| | Water area | 0 | 0 | 0 | 0 | — | 0 | 0 | 0 |
| | Wetland | 0 | 0 | 0 | 0 | 0 | — | 0 | 0 |
| | Construction land | 0 | 0 | 0 | 0 | 0 | 0 | — | 0 |
| | Unused land | 25 | 10 | 0 | 0 | 0 | 0 | 1 | — |

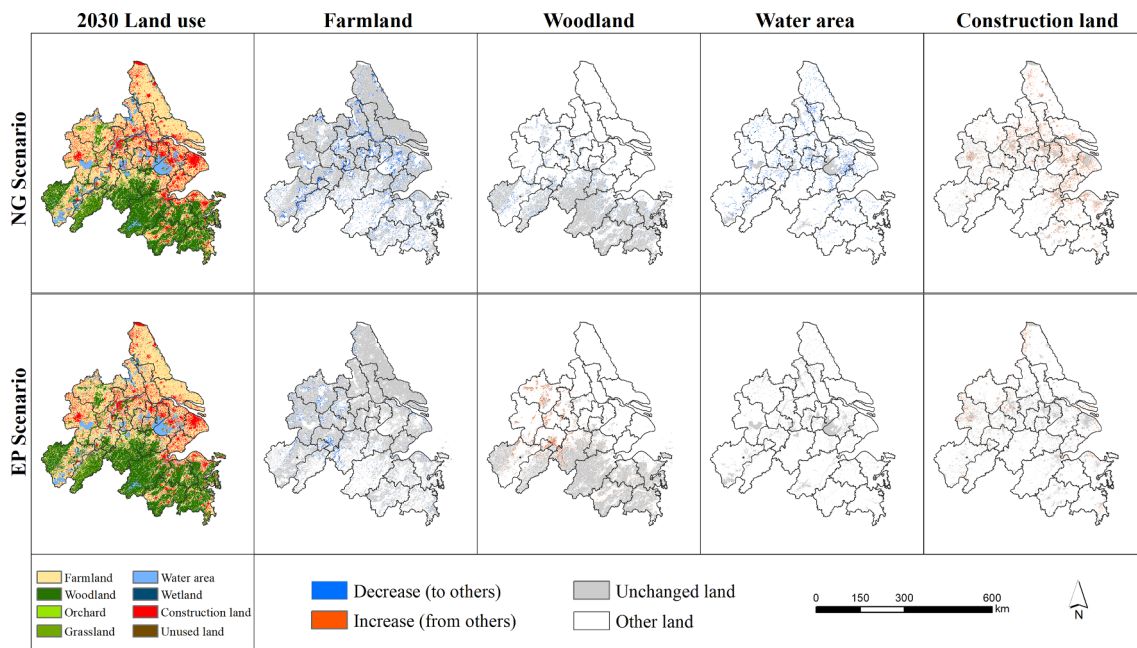


Fig. 6. Spatial distributions of predicted land use/cover in 2030 and the change of farmland, woodland, water area and construction land for 2015–2030 under natural growth (NG) and ecological protection (EP) scenarios.

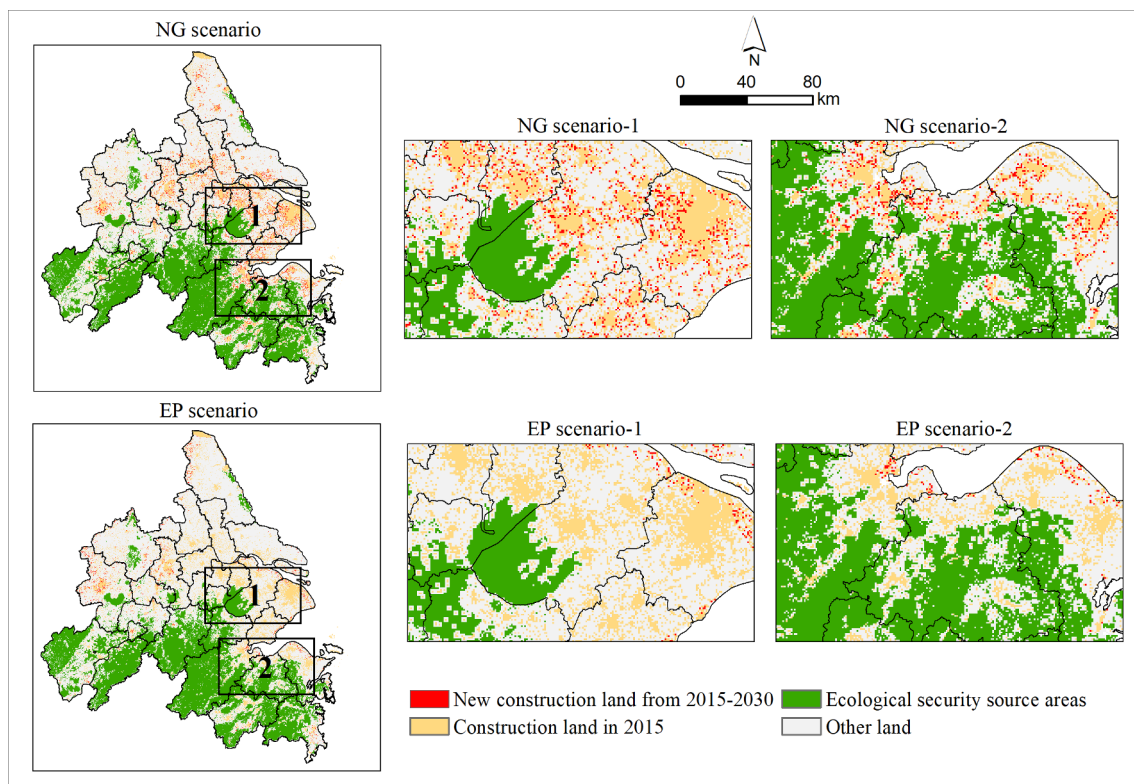


Fig. 7. The simulated new construction land overlaid with ESSA from 2015 to 2030 under NG and EP scenarios.

policies in any natural-resource decision-making process.

The second limitation is the lack of scientific threshold determination of ESSA. In other words, the optimal area of ESSA should be determined. In this study, the natural break point method was used for classification, and the ecological patches with higher importance were extracted as ESSA. However, whether the area of ESSA can meet the regional ecological needs is uncertain. Moreover, there is a slight gap between the results of this study and the current regional planning. The

existing regional planning, DP-YRD, divides the territorial space of the YRD into three types: optimized development area, key development area and restricted development area. Restricted development areas designated by DP-YRD account for 48% of the total area and are mainly distributed in northern Jiangsu, western Anhui and western Zhejiang. By comparing the ESSA with restricted development areas, we observed that although the spatial distribution of ESSA is consistent with that of the restricted development areas, ESSA are 16% smaller than the

restricted development areas. Therefore, scientific determination of the area threshold of ESSA needs to be further studied and improved.

The third limitation is the limited settings of the land use prediction scenarios for future development planning reference in the YRD. In the simulations, to highlight the role of ecological protection, only two scenarios were conducted in this study. In fact, besides ecological security, food security is also important to support societal development. Ecological security, food security and economic development should be simultaneously considered in regional development efforts. However, the ecological protection scenario in this study does not reflect the real-life trade-off between farmland protection and ecological security. Hence, a method to balance and coordinate farmland protection, ecological protection and economic development should be explored through scenario simulations.

5.2. Land use simulation incorporating ecological security

Previous studies have discussed the impacts of land use on the ecosystems; however, prevention is more important than post-destruction management. An increasing number of countries and regions began to emphasize the importance of planning and policy-making to minimize the negative impacts of land use changes on ecology to ensure ecological security (Liu and Chang, 2015). Rapid population growth requires more construction land. However, the speed of construction land expansion has exceeded the growth rate of the urban population in China at the cost of ecological land (Zhang et al., 2016). Thus, it is urgent to prevent the conversion from ecological land to other land uses. The problem lies in the determination of the priority protected areas. In this study, we developed a land use prediction framework combined with the comprehensive identification of ESSA. Through this approach, areas that are critical for ecological security can be reasonably positioned and land use patterns can be optimized under the premise of ecological protection, which is of great significance for land use spatial planning and decision-making.

ESSA are considered critical areas to protect ecosystem stability and biodiversity. Some studies have identified ESSA through ecosystem services and landscape connectivity (Zhang et al., 2016) or habitat quality and landscape connectivity (Peng et al., 2018). However, incomplete consideration cannot reflect the comprehensive function and importance of ESSA in safeguarding ecological security. Compared with the previous studies, this study constructs a more comprehensive evaluation framework of ESSA based on the three connotative objectives of ecological security. Habitat quality corresponds to the goal of preventing ecological degradation, and the importance of ecosystem services is related to the sustainability of ecosystem services, and landscape connectivity focuses on ecosystem integrity. Through this three-dimensional consideration, ESSA can be used for ecological evaluation and ecological environmental planning.

5.3. Advantages of the future land use simulation model

In land use simulation, most studies adopt the logistic regression to analyze the relationships between natural and socioeconomic spatial variables with land use patterns, which are typically used in the CLUE model (Wang et al., 2018; Zhou et al., 2016). This method cannot address the non-linear relationship between independent driving factors and land use change. The ANN is a machine learning model and generally used to approximate non-linear functions consisting of various independent variables. The advantage of ANN lies in its capability of fitting complex relationships between inputs and training objectives through a series of iterative learning and memory (Liu et al., 2017). Moreover, ANN can yield ideal performance when modeling a variety of inputs and outputs. The FLUS model embeds ANN into the probability estimation module to calculate the probability of occurrence of each land use type on a specific grid. It is capable of addressing the complicated relationships between the driving factors and land use change

using machine learning and is more effective than logistic regression.

5.4. Possible innovation of landscape connectivity analysis

The PC indicator has been widely used to evaluate landscape connectivity (Ernst, 2014; Ng et al., 2013; Nogués and Cabarga-Varona, 2014). However, the traditional method of only using the PC index has some limitations. On the one hand, landscape connectivity at the patch level ignores the connectivity between patches; on the other hand, the running time in Conefor increases rapidly with the growing number of nodes and links, especially for the PC indicator. The MSPA based on the mathematical morphological operations method can identify the habitat patches with high connectivity at the pixel level and does not require the identification of individual patches. Besides, the landscape types identified by MSPA are not affected by the large spatial scale. Therefore, we integrated MSPA with PC analysis to assess landscape connectivity and improve the efficiency and effectiveness of the calculation process. This combined method cannot only improve the computational efficiency of the PC indicator, but also make it possible to evaluate landscape connectivity on a large scale by combining the evaluations at the pixel level and patch level.

6. Conclusions

Since the end of the 20th century, with the rapid development of urbanization, ecological space in the YRD has been gradually eroded. Moreover, due to the excessive exploitation and utilization of natural resources, ecological and environmental problems have become increasingly prominent in the YRD. The land use change from 2010 to 2015 reveals the expansion of construction land at the expense of ecological land. About 1.3% of the ecological land has been lost, whereas construction land expanded by 2373 km². This development pattern will continue to disturb the entire ecosystems.

This study aims to explore the trends in the land use change constrained by ecological security source areas (ESSA). The identification of ESSA is a critical step in land use simulations based on ecological security. The multi-perspective ESSA identification, considering habitat quality, ecosystem services and landscape connectivity, reflects various connotative objectives of ecological security. The FLUS model embedded with ANN is a good fit to calculate the complex relationships between selected driving factors and land use change. The selection of driving factors in this study covers a variety of aspects such as geographical, climatic, economic and social factors. The overall accuracy of the simulation with the FLUS model is over 87%.

The results show that the important ecological protected areas in the YRD are 64,911 km², accounting for 32.51% of the total area, mainly distributed in southern Anhui, western Zhejiang, Taihu Lake and Chaohu Lake. Through the delineation of ESSA, 159 km² of woodland, 150 km² of orchard, 523 km² of water area and 98 km² of wetland are protected; in addition, the growth of the construction land slows down and all new construction land is located outside the ESSA under ESSA-based EP. In order to achieve the goal of ecological protection, stakeholders and government decision makers should formulate and implement relevant protection policies, including promptly delimiting the ESSA, strictly controlling the occupation of natural forestry and wetlands, protecting the water quality and quantity of water sources and strengthening the construction of green infrastructure.

Although this study discusses the impact of ESSA on land use changes, it is insufficient to predict the land use demand area under different scenarios. Land use demand area prediction is an important link in land use planning. The overall land use quantity structure determines the macroscopic balance between humans and nature, followed by the spatial balance in different regions. Land use planning based on a reasonable land use demand is beneficial to the sustainable development of the society. Therefore, a stronger time prediction model such as the system dynamic (SD) model should be combined with the

proposed land use projection framework in future work. Besides, this study is limited to predicting future land use based on current time-driven factor data. More accurate projection of future socio-economic and climatic scenarios can help us better simulate and predict future land use. Thus, further study is needed to simulate future land use under different scenarios through future social, economic, demographic, geographical and climatic conditions to improve the spatial-temporal prediction ability of the model guide planning and policy efforts.

CRedit authorship contribution statement

Dou Zhang: Conceptualization, Methodology, Writing - original draft. **Xiangrong Wang:** Resources, Project administration, Funding acquisition. **Liping Qu:** Formal analysis, Conceptualization. **Shicheng Li:** Supervision, Writing - review & editing. **Yuanping Lin:** Software, Investigation, Visualization. **Rui Yao:** Resources, Validation. **Xiao Zhou:** Data curation, Supervision. **Jingye Li:** Software, Methodology.

Declaration of Competing Interest

The authors declare that they have no known competing financial interests or personal relationships that could have appeared to influence the work reported in this paper.

Acknowledgements

This research is funded by the National Key Research and Development Program of China (2016YFC0502705), the National natural science foundation of China (41871172), the Ministry of Land and Resources Key laboratory for land use open foundation of China (KLLU201704) and Key Laboratory of Meteorological Disaster of Ministry of Education, Nanjing University of Information Science and Technology (No. KLME1506). Also, the authors are grateful to the Data Center for Resources and Environmental Sciences, Chinese Academy of Sciences (<http://www.resdc.cn>), Science and Technology Resource Service System of National Ecosystem Observation and Research Network (<http://www.cern.org.cn>), China Economic and Social Development Statistical Database (<http://tongji.cnki.net>), and Specimen Resource Sharing Platform of China Nature Reserve (<http://www.papc.cn>) for the access to the spatial data.

References

Aburas, M.M., Ho, Y.M., Ramli, M.F., Ash'aari, Z.H., 2017. Improving the capability of an integrated CA-Markov model to simulate spatio-temporal urban growth trends using an Analytical Hierarchy Process and Frequency Ratio. *Int. J. Appl. Earth Obs. Geoinf.* 59, 65–78.

Commission, N.D.a.R., 2016. Development Plan of Yangtze River Delta Urban Agglomerations from 2010 to 2030, <http://zfxgk.ndrc.gov.cn/web/iteminfo.jsp?id=358>.

Costanza, R., de Groot, R., Sutton, P., van der Ploeg, S., Anderson, S.J., Kubiszewski, I., Farber, S., Turner, R.K., 2014. Changes in the global value of ecosystem services. *Global Environ. Change* 26, 152–158.

Ernst, B.W., 2014. Quantifying connectivity using graph based connectivity response curves in complex landscapes under simulated forest management scenarios. *For. Ecol. Manage.* 321, 94–104.

Geijzendorffer, I.R., Cohen-Shacham, E., Cord, A.F., Cramer, W., Guerra, C., Martín-López, B., 2017. Ecosystem services in global sustainability policies. *Environ. Sci. Policy* 74, 40–48.

Gong, S.H., Xiao, Y., Zheng, H., Xiao, Y., Ouyang, Z.Y., 2017. Spatial patterns of ecosystem water conservation in China and its impact factors analysis. *Acta Ecologica Sinica* 37, 2455–2462.

Guo, R., Wu, T., Liu, M., Huang, M., Stendardo, L., Zhang, Y., 2019. The Construction and Optimization of Ecological Security Pattern in the Harbin-Changchun Urban Agglomeration. *Int J Environ Res Public Health*, China, pp. 16.

Hall, L.S., Krausman, P.R., Morrison, M.L., 1997. The habitat concept and a plea for standard terminology. *Wildlife Soc B* 25, 173–182.

Hu, W.S., Wang, S.S., Li, D.H., 2010. Biological conservation security patterns plan in Beijing based on the focal species approach. *Acta Ecologica Sinica* 30, 4266–4276.

Huang, Q., Wang, R., Ren, Z., Li, J., Zhang, H., 2007. Regional ecological security assessment based on long periods of ecological footprint analysis. *Resour. Conserv.*

Recycl. 51, 24–41.

Islam, K., Rahman, M.F., Jashimuddin, M., 2018. Modeling land use change using Cellular Automata and Artificial Neural Network: The case of Chunati Wildlife Sanctuary, Bangladesh. *Ecol. Ind.* 88, 439–453.

Jiang, B., Bai, Y., Wong, C.P., Xu, X., Alatalo, J.M., 2019. China's ecological civilization program—Implementing ecological redline policy. *Land Use Policy* 81, 111–114.

Jin, G., Chen, K., Wang, P., Guo, B., Dong, Y., Yang, J., 2019. Trade-offs in land-use competition and sustainable land development in the North China Plain. *Technol. Forecast. Soc. Chang.* 141, 36–46.

Jin, G., Deng, X., Zhao, X., Guo, B., Yang, J., 2018. Spatiotemporal patterns in urbanization efficiency within the Yangtze River Economic Belt between 2005 and 2014. *J. Geog. Sci.* 28, 1113–1126.

Kadavi, P.R., Lee, C.-W., 2018. Land cover classification analysis of volcanic island in Aleutian Arc using an artificial neural network (ANN) and a support vector machine (SVM) from Landsat imagery. *Geosci. J.* 22, 653–665.

Kang, J., Fang, L., Li, S., Wang, X., 2019. Parallel Cellular Automata Markov Model for Land Use Change Prediction over MapReduce Framework. *ISPRS Int. J. Geo-Inf.* 8, 454.

Kong, F., Yin, H., Nakagoshi, N., Zong, Y., 2010. Urban green space network development for biodiversity conservation: Identification based on graph theory and gravity modeling. *Landscape Urban Plann.* 95, 16–27.

Li, S., Bing, Z., Jin, G., 2019. Spatially Explicit Mapping of Soil Conservation Service in Monetary Units Due to Land Use/Cover Change for the Three Gorges Reservoir Area. *China. Remote Sensing* 11, 468.

Li, S., Xiao, W., Zhao, Y., Lv, X., 2020. Incorporating ecological risk index in the multi-process MCRE model to optimize the ecological security pattern in a semi-arid area with intensive coal mining: A case study in northern China. *J. Cleaner Prod.* 247, 119143.

Li, S., Zhang, Y., Wang, Z., Li, L., 2018. Mapping human influence intensity in the Tibetan Plateau for conservation of ecological service functions. *Ecosyst. Serv.* 30, 276–286.

Li, Y., Liu, C., Min, J., Wang, C., Zhang, H., Wang, Y., 2013. RS/GIS-based integrated evaluation of the ecosystem services of the Three Gorges Reservoir area (Chongqing section). *Acta Ecologica Sinica* 33, 11.

Liang, X., Liu, X., Li, X., Chen, Y., Tian, H., Yao, Y., 2018. Delineating multi-scenario urban growth boundaries with a CA-based FLUS model and morphological method. *Landscape Urban Plann.* 177, 47–63.

Lin, Y., Deng, X., Li, X., Ma, E., 2014. Comparison of multinomial logistic regression and logistic regression: which is more efficient in allocating land use? *Frontiers of Earth Science* 8.

Liu, D., Chang, Q., 2015. Ecological security research progress in China. *Acta Ecologica Sinica* 35, 111–121.

Liu, M., Hu, Y., Zhang, W., Zhu, J., Chen, H., Xi, F., 2011. Application of land-use change model in guiding regional planning: A case study in Hun-Taizi River Watershed, Northeast China. *Chinese Geographical Science* 21, 609–618.

Liu, X., Liang, X., Li, X., Xu, X., Ou, J., Chen, Y., Li, S., Wang, S., Pei, F., 2017. A future land use simulation model (FLUS) for simulating multiple land use scenarios by coupling human and natural effects. *Landscape Urban Plann.* 168, 94–116.

Lu, Q., Chang, N.-B., Joyce, J., Chen, A.S., Savic, D.A., Djordjevic, S., Fu, G., 2018. Exploring the potential climate change impact on urban growth in London by a cellular automata-based Markov chain model. *Comput. Environ. Urban Syst.* 68, 121–132.

Luo, J., Zhan, J., Lin, Y., Zhao, C., 2014. An equilibrium analysis of the land use structure in the Yunnan Province. *China. Frontiers of Earth Science* 8, 12.

Ma, L., Bo, J., Li, X., Fang, F., Cheng, W., 2019. Identifying key landscape pattern indices influencing the ecological security of inland river basin: The middle and lower reaches of Shule River Basin as an example. *Sci. Total Environ.* 674, 424–438.

Ng, C.N., Xie, Y.J., Yu, X.J., 2013. Integrating landscape connectivity into the evaluation of ecosystem services for biodiversity conservation and its implications for landscape planning. *Appl. Geogr.* 42, 1–12.

Nogués, S., Cabarga-Varona, A., 2014. Modelling land use changes for landscape connectivity: The role of plantation forestry and highways. *Journal for Nature Conservation* 22, 504–515.

Peng, J., Pan, Y., Liu, Y., Zhao, H., Wang, Y., 2018. Linking ecological degradation risk to identify ecological security patterns in a rapidly urbanizing landscape. *Habitat International* 71, 110–124.

Petrosillo, I., Zaccarelli, N., Semeraro, T., Zurlini, G., 2009. The effectiveness of different conservation policies on the security of natural capital. *Landscape Urban Plann.* 89, 49–56.

Posner, S., Verutes, G., Koh, I., Denu, D., Ricketts, T., 2016. Global use of ecosystem service models. *Ecosyst. Serv.* 17, 131–141.

Qiu, L., Pan, Y., Zhu, J., Amable, G.S., Xu, B., 2019. Integrated analysis of urbanization-triggered land use change trajectory and implications for ecological land management: A case study in Fuyang, China. *Sci. Total Environ.* 660, 209–217.

Saura, S., Pascual-Hortal, L., 2007. A new habitat availability index to integrate connectivity in landscape conservation planning: Comparison with existing indices and application to a case study. *Landscape Urban Plann.* 83, 91–103.

Shi, P., Yu, D., 2014. Assessing urban environmental resources and services of Shenzhen, China: A landscape-based approach for urban planning and sustainability. *Landscape Urban Plann.* 125, 290–297.

Soille, P., Vogt, P., 2009. Morphological segmentation of binary patterns. *Pattern Recogn. Lett.* 30, 456–459.

Teng, M., Wu, C., Zhou, Z., Lord, E., Zheng, Z., 2011. Multipurpose greenway planning for changing cities: A framework integrating priorities and a least-cost path model. *Landscape Urban Plann.* 103, 1–14.

Velázquez, J., Gutiérrez, J., Hernando, A., García-Abril, A., 2017. Evaluating landscape connectivity in fragmented habitats: Cantabrian capercaillie (*Tetrao urogallus*

- cantabricus) in northern Spain. *For. Ecol. Manage.* 389, 59–67.
- Verburg, P.H., Soepboer, W., Veldkamp, A., Limpiada, R., Espaldon, V., Mastura, S.S., 2002. Modeling the spatial dynamics of regional land use: the CLUE-S model. *Environ. Manage.* 30, 391–405.
- Wang, S., Zhang, X., Wu, T., Yang, Y., 2019. The evolution of landscape ecological security in Beijing under the influence of different policies in recent decades. *Sci. Total Environ.* 646, 49–57.
- Wang, Y., Li, X., Zhang, Q., Li, J., Zhou, X., 2018. Projections of future land use changes: Multiple scenarios-based impacts analysis on ecosystem services for Wuhan city, China. *Ecol. Ind.* 94, 430–445.
- Wood, S.L.R., Jones, S.K., Johnson, J.A., Brauman, K.A., Chaplin-Kramer, R., Fremier, A., Girvetz, E., Gordon, L.J., Kappel, C.V., Mandel, L., Mulligan, M., O'Farrell, P., Smith, W.K., Willemen, L., Zhang, W., DeClerck, F.A., 2018. Distilling the role of ecosystem services in the Sustainable Development Goals. *Ecosyst. Serv.* 29, 70–82.
- Wu, J.S., Zhang, L.Q., Peng, J., Feng, Z., Liu, H.M., He, S.B., 2013. The integrated recognition of the source area of the urban ecological security pattern in Shenzhen. *Acta Ecologica Sinica* 33, 4125–4133.
- Xiao, Y., Ouyang, Z., Xu, W., Xiao, Y., Xiao, Q., 2015. GIS-based spatial analysis of soil erosion and soil conservation in Chongqing, China. *Acta Ecologica Sinica* 35, 9.
- Yao, G., Xie, H., 2016. Rural spatial restructuring in ecologically fragile mountainous areas of southern China: A case study of Changgang Town, Jiangxi Province. *Journal of Rural Studies* 47, 435–448.
- Yao, R., Wang, L.C., Huang, X., Gong, W., Xia, X.G., 2019. Greening in Rural Areas Increases the Surface Urban Heat Island Intensity. *Geophys Res Lett* 46, 2204–2212.
- Yu, K., Wang, S., Li, D., Li, C., 2009. The function of ecological security patterns as an urban growth framework in Beijing. *Acta Ecologica Sinica* 29, 16.
- Zhang, L., Peng, J., Liu, Y., Wu, J., 2016. Coupling ecosystem services supply and human ecological demand to identify landscape ecological security pattern: A case study in Beijing–Tianjin–Hebei region, China. *Urban Ecosystems* 20, 701–714.
- Zhou, R., Zhang, H., Ye, X.-Y., Wang, X.-J., Su, H.-L., 2016. The Delimitation of Urban Growth Boundaries Using the CLUE-S Land-Use Change Model: Study on Xinzhuang Town, Changshu City, China. *Sustainability* 8, 1182.